Passive UHF RFID Antennas for Sensing Applications: Principles, Methods and Classifications

C. Occhiuzzi, S. Caizzone and G. Marrocco

January 7, 2013

Pre-Print

Please cite as

C. Occhiuzzi, S. Caizzone, G. Marrocco, "Passive UHF RFID Antennas for Sensing Applications: Principles, Methods and Classifications", *IEEE Antennas and Propagation Magazine*, Feb. 2014.

Passive UHF RFID Antennas for Sensing Applications: Principles, Methods and Classifications

C. Occhiuzzi, S. Caizzone and G. Marrocco

January 7, 2013

Abstract

UHF passive Radio Frequency Identification technology is rapidly evolving from simple labeling of things to wireless pervasive sensing. A remarkable number of scientific papers demonstrate that objects could be in principle remotely tracked and monitored in their physical properties all along their life-cycle. The key background is a new paradigm of antenna design that merges together the conventional communication issues with more specific requirements about sensitivity to time-varying boundary conditions. This paper presents a unified review on the state of the art about the tag-as-sensor problem with particular care to formalize the measurement indicators and the communication and sensing trade-off, with the purpose to provide a first knowledge base to face a large variety of emerging sensing applications.

Key Words: RFID, Antennas, sensors, Internet of Things.

1 Introduction

Radio Frequency Identification (RFID) is nowadays a well assessed technology for tracking goods and trace procedures with several advantages over barcode systems [1]. More complex applications are currently researched worldwide in many university laboratories concerning sensing, localization, other frequency bands, new materials, and more efficient communication protocols. The sensing capabilities offered by passive RFID tags in the UHF bands are perhaps the most exciting research trend, with great applicability to the emerging paradigm

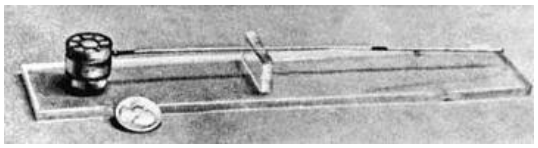

Figure 1: Theremin's bug (1945), the first passive radio sensor converting voice pressure into a modulation of the radar cross-section of a wire antenna through a capacitor microphone.

of Internet of Things [2]. A "swarm" [3] of low-cost tiny interconnected sensors interacting with the nearby environment will enable an augmented perception of the reality stimulating improvements of the **well-being** as well as completely new services. For such forthcoming applications, spatial granularity is a key concept [4]. Because of their intended massive use, sensors need not to be extremely sophisticated or precise; **at the same time, however,** they are demanded to satisfy low-cost requirements in order to be deployed at finer granularity than active precise wireless systems. The ultimate goal is to design "smart dust motes" [5], i.e. autonomous sensing, computing and communication systems small enough to be easily "dispersed in the environment". In order to enable such vision, passive UHF RFID technology can play a strategic role, thanks to its low-cost, wireless and "sensing-friendly" capabilities.

The use of an antenna as part of a passive sensor is not new and occurred much before the appearance of RFID microchips. In the late 1940s the Russian inventor Leon Theremin [6] developed one of the first covert listening devices (the "bug") using a capacitor microphone connected to an antenna (Fig.1) to transmit away, through reflection of an interrogating carrier, the audio signals captured in nearby environments.

On approaching our times, the unique feature of the RFID microchip modulators further adds a completely new sensing possibility by taking into consideration that RFID tags are tiny computers of increasing performance with tiny low-power radios which merge together both digital (the microchip and binary data generation) and analog (antennas and propagation phenomenology) features. Data transmitted back to the reader during the interrogation protocol are digitally encoded, but the strength of the backscattered power is governed in an analog manner by the interaction with nearby objects, by the propagation modality, and even by the mutual position and orientation among reader and tags. This fact poses the basis for a different sensing modality wherein the captured data can be even collected by a "sensor-less" tag, just by exploiting the

physics of the RFID response.

In the last 3-5 years, a remarkable number of scientific papers demonstrated, at different level of maturity and for different applications, that the passive RFID sensing could be affordable with the available manufacturing technology, while an important effort is still required to fully understand and to manage the physics of RFID sensing and evolve from isolated laboratory experiments to first stable and self-consistent products. In particular, a systematization of phenomena, metrics and system parameters is of prominent relevance to provide tools to evaluate the true performance of the tag as a sensor and make comparison among different implementations.

Thus, following the style of a previous paper of the same authors [7], wherein the basic design options for general-purpose UHF tags were described in a unitary way, and starting from the more recent contribution in [8], the present work tries to systematize the different declinations of UHF RFID **antennas for passive sensors**, with particular care to clarify the relationships and constraints for communication and sensing and introduce performance parameters of general application.

The paper is organized as follows. Section II introduces the parameters that can be measurable by RFID readers and some possible metrics relating measurements to the process under observation. Section III discusses about the co-habitation between the performance of a tag as a sensor and the constraints over the required reading distance and introduces an overall communication-sensing nomogram. Section IV describes the class of *bare* tags whose sensing capability is only related to the natural sensitivity of an antenna to time-variant boundary conditions, while kinds of *loaded* tag including specific chemical and mechanical sensor loads are analyzed in Section V. Section VI finally shows the achievable resolution of the whole tag-reader system depending on the kind of used metrics. To complete the analysis, a quick overview on the new emerging sensing paradigms is finally given in Section VI.

Theoretical discussions and classifications are corroborated by many examples taken from recent scientific literature.

2 Measurable data and metrics

An RFID system comprises two components: the remote transponder or *tag*, including an antenna and a microchip transmitter **(IC)**, located on the object

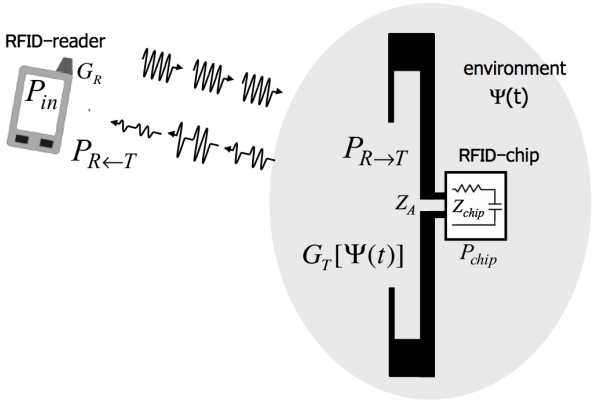

Figure 2: Sketch of the RFID sensing system: a reader interrogates the tag, whose behavior is influenced by a changing physical feature Ψ.

Table 1: Worldwide UHF band and power limitations

Country	band (MHz)	max EIRP (W)
Europe	866-869	3.2
USA	902-928	4.0
Japan	950-956	4.0

to be identified, and the local querying system or *reader*, which can collect data transmitted from the tag (Fig.2), eventually performing a first processing job. Various kinds of data, and first of all a unique identification code (ID), can be wirelessly transferred to the reader by means of radio-frequency electromagnetic signals.

The tags could be *passive*, harvesting energy from the interrogating system, *semi-active* when a battery is included only to feed the sensors, or *fully active* where a local source directly feeds a micro controller as well as the transmitting radio. This work is focused on passive systems, which may have an almost unlimited life and very low cost. Among the actual options, the most attractive standard is the UHF band (frequency allocations and maximum power emission in Tab.I), which in principle promises activation ranges up to 10 meters.

In *passive* technology, at the beginning of the reader-to-tag communication protocol [9], the reader first activates the tag, placed over a target object, by sending a continuous wave, which, by charging an internal capacitor, provides the required energy to perform actions. During this *listening mode*, the mi-

crochip exhibits an input impedance $Z_{chip} = R_{chip} + jX_{chip}$, with X_{chip} being capacitive. The antenna impedance $Z_A = R_A + jX_A$ has to be matched to Z_{chip} ($Z_A = Z^*_{chip}$) for maximum power transfer (a comprehensive review of the techniques to match the antenna with the chip is provided in [7]). During the next steps of the communication, the tag receives commands from the reader and finally sends back the data through a *backscattered modulation* of the continuous wave provided by the reader itself. In this case, the tag's IC acts as a programmable switching device between a low impedance and a high impedance, thus modifying the reflectivity of the responding tag, and hence the strength of the reflected power.

2.1 Measurable parameters

In order for a tag to monitor physical parameters, a sensing functionality needs to be added, either physically or just logically. Before going into a particular sensing problem, it is hence useful to introduce the basic RFID e.m. parameters suitable to sensing purposes. A single-chip configuration is considered throughout the paper, but the same ideas may be nonetheless extended to the multi-chip systems recently introduced in [10-11-12].

Let's denote with $\Psi(t)$ a local physical, chemical or geometrical parameter of the environment surrounding the tag (**the Sensor-tag, hereafter *S-tag*)** which has to be monitored by the RFID platform. According to the specific applications, Ψ could be the presence of gases and chemical species able to react with the sensitive materials integrated into the antenna, a physical stimulus, e.g. an acceleration able to affect a discrete sensor loading the RFID tag, a shape factor of a biological process, the temperature of the environment or the local effective permittivity "sensed" by the tag's antenna.

Sensing indicators can be easily derived from data measurable by the reader. At this purpose, the equations of two-way reader-tag link [13] need to be rewritten making explicit the dependence on the variation of local parameters [8]. Under the simplifying hypothesis of free-space interactions, the power collected at the microchip (1) and the power backscattered by the tag toward the reader (2), and collected by it, are the following:

$$P_{R\to T}[\Psi] = \left(\frac{\lambda_0}{4\pi d}\right)^2 P_{in} G_R(\theta,\phi) G_T[\Psi](\theta,\phi)\tau[\Psi]\eta_p \qquad (1)$$

$$P_{R\leftarrow T}[\Psi] = \frac{1}{4\pi}\left(\frac{\lambda_0}{4\pi d^2}\right)^2 P_{in} G_R^2(\theta,\phi)\eta_p^2 rcs_T[\Psi(\theta,\phi)] \tag{2}$$

where d is the reader-tag distance, G_R is the gain of the reader antenna, $G_T[\Psi]$ is the gain of the tag's antenna at the specific realization of the process. P_{in} is the power entering the reader's antenna**,** η_p is the polarization mismatch between the reader and the tag, and $\tau[\Psi]$ is the power transmission coefficient of the tag :

$$\tau[\Psi] = \frac{4R_{chip}R_a[\Psi]}{|Z_{chip} + Z_a[\Psi]|^2} \tag{3}$$

rcs_T is finally the tag's radar cross-section, related to the modulation impedance Z_{mod} of the microchip to encode the low and high digital state:

$$rcs_T[\Psi] = \frac{\lambda_0^2}{4\pi} G_T^2[\Psi](\theta,\phi)\left(\frac{2R_a[\Psi]}{|Z_{mod} + Z_a[\Psi]|}\right)^2 \tag{4}$$

The backscattered power $P_{R\leftarrow T}$ is measurable (Fig.3a) by the reader in terms of Received Signal Strength Indicator (RSSI), here assumed to correspond [13,14] to the binary modulating state having $Z_{mod} = Z_{chip}$.

Another parameter that can be measured by the reader is the *turn-on power* $P_{in}^{to}[\Psi]$, e.g. the minimum input power P_{in} through the reader's antenna forcing the tag to respond (Fig.3b). It can be derived from (1) by considering $P_{R\rightarrow T} = P_{chip}$, with the latter being the microchip sensitivity:

$$P_{in}^{to}[\Psi] = (\frac{\lambda_0}{4\pi d})^{-2}\frac{P_{chip}}{G_R(\theta,\phi)\eta_p G_T[\Psi](\theta,\phi)\tau\,[\Psi]} \tag{5}$$

From turn-on measurement it is possible to extract by proper calibration [15] the *realized gain* of the tag $\hat{G}_T = G_T\tau$, e.g. the gain of the tag scaled by the mismatch to the IC.

Finally, forward (1) and backward (2) powers may be combined at turn-on condition with the purpose to drop out the influence of the distance and of the reader's and tag's gains and orientation [11,12]. A non-dimensional indicator (Fig.3c), denoted as *Analog Identifier* (AID), can be hence introduced:

$$AID[\Psi] = \frac{P_{chip}}{\sqrt{P_{R\leftarrow T}[\Psi]P_{in}^{to}[\Psi]}} = \frac{2R_{chip}}{|Z_{chip} + Z_a\,[\Psi]|} \tag{6}$$

AID only depends on the antenna impedance and thus it appears useful when

the interrogation set-up changes (position and orientation) in successive measurements since it is immune to the interrogation modalities.

Other kinds of direct metrics may be defined, just like the differential reflection coefficient in [16] which even accounts for the different response of the antenna in the two modulating states.

2.2 Sensing Metrics

The indicators in (2), (5), and (6), may be used as *data inversion curves* between the measured data and the evolution $\Psi(t)$ of the process:

$$\{AID, P_{in}^{to}, P_{T\rightarrow R}\} \leftrightarrow \Psi(t) \tag{7}$$

It could be useful to normalize each indicator by its value in a particular reference state, say Ψ_0, for instance collected at the time of the tag placement into the environment to be monitored. The normalized parameters are hereafter generically indicated with $\xi[\Psi]$. They can be collected at a fixed frequency or instead within the whole RFID band to provide integral metrics suitable to capture macroscopic variations of the S-tag response over frequency such as the detuning and the attenuation or magnification of the response (Fig.3 d,e). The *frequency shift*, e.g. the frequency correlation distance Δf between $\xi[\Psi](f)$ and the initial response $\xi[\Psi_0](f)$

$$\Delta f[\Psi] : \int_{f_1}^{f_2} \xi[\Psi]_0(f) \cdot \xi[\Psi](f+\Delta f)df \quad \textbf{is maximum} \tag{8}$$

gives a measure of the change of the antenna resonance due to the evolving chemical-physical process. The *scale factor*

$$\gamma[\Psi] = \frac{\int_{f_1}^{f_2} |\xi[\Psi](f-\Delta f) - \xi[\Psi_0](f)|df}{\int_{f_1}^{f_2} |\xi[\Psi_0](f)|df} \tag{9}$$

describes instead the overall attenuation/amplification of the S-tag response. These two indicators look particularly useful in those Countries wherein the available bandwidth for UHF RFID is significant, such as USA. Their application is less effective in Europe due to the very modest allowed bandwidth.

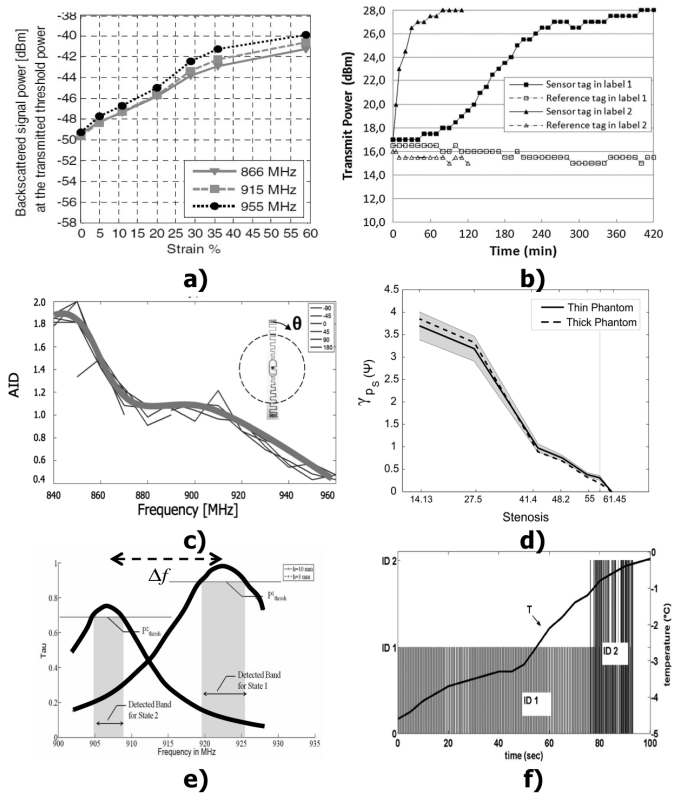

Figure 3: Examples of measured sensing indicators. a) backscattered power vs. strain [17]; b) turn-power vs. Humidity [18]; c) Analog identifier measured at different observation angles [12]; d) Integral metrics: scale factor [19]; e) Integral metrics: frequency shift [20] f) Binary detection of temperature threshold [21]

As for usual sensors, the response of the S-tag can be quantified by the *dynamic range,* e.g. the overall change of the measured parameters between the extreme interesting realizations of the process, Ψ_{min}, Ψ_{max}, conveniently expressed in decibel

$$\Delta\xi = |\xi[\Psi_{max}] - \xi[\Psi_{min}]|_{dB} \tag{10}$$

and by means of the *Sensitivity*

$$S\left[\xi\right] = \frac{\partial\xi[\Psi]}{\partial\Psi} \tag{11}$$

If the S-tag response is approximately linear in the useful range of the process, hence

$$S\left[\xi\right] \simeq \frac{\Delta\xi}{\Psi_{max} - \Psi_{min}} \tag{12}$$

The sensitivity and the dynamic range of the system are thus strictly connected to the antenna's features, in particular to its quality factor, and definitely to its bandwidth. On considering the whole reader/S-tag system, the overall performance parameter is the *Resolution* which accounts **also** for the discretization of the reader's signals. This topic is of prominent importance for the true real applicability of S-tags and will be addressed later on in a dedicated section.

3 Communication and Sensing Trade-off

Sensing capabilities are generally achieved at the expenses of read-distance degradation since the change of physical/chemical features of the environment are sensed by the **passive** tag through a deviation from its static gain and/or impedance matching. Hence the true effectiveness of an S-tag results from the trade-off between sensing and communication [19].

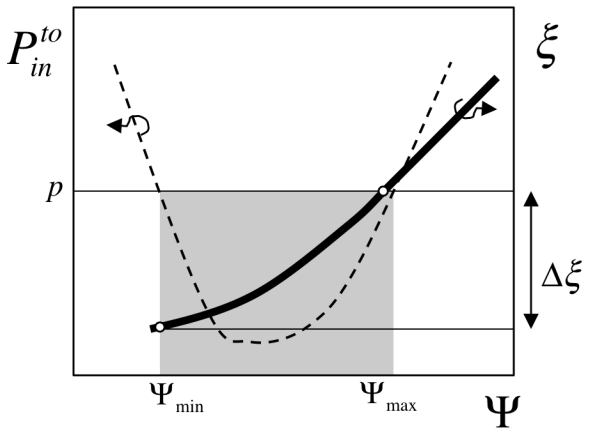

Figure 4: Pictorial relationship between the maximum sensing dynamic range $\Delta\xi$ of an S-tag and the constrains over the maximum power p emitted by the reader.

3.1 Constraints

Sensing requirements induce a constraint over the dynamic range:

$$\Delta\xi \geq R \tag{13}$$

with R is the requested span of the measured data. Preserving a useful read range in all the states of the process means instead enforcing a condition over the minimum turn-on power (see Fig.4)

$$P_{in}^{to}(\Psi) \leq p \quad \Psi_{min} \leq \Psi \leq \Psi_{max} \tag{14}$$

The power bound p has to comply with the local regulations (Tab.I) and with the true available power for fixed or hand-held readers. Having selected the reader-tag distance, such a constrain will enforce, from (5), the minimum allowed value for the realized gain all along the process:

$$G_T(\Psi)\tau(\Psi) \geq g \quad for \quad \Psi_{min} \leq \Psi \leq \Psi_{max} \tag{15}$$

It is worth noticing that an S-tag can be turned into a detector of a particular state Ψ_k of the process if the antenna is really narrowband so that condition (14) holds just in the close surrounding of Ψ_k, e.g. $|\Psi_{max} - \Psi_{min}| \to 0$ in Fig.4. A discrete set of events of the process may be hence recognized by using a multiplicity of tags or a single multi-port tag (Fig.3f), with different impedance matching conditions, as described in [10]. Each event Ψ_k to be recognized is accordingly linked to the ID_k of the microchip which has scavenged enough power to interact with the reader ($P_{k,in}^{to}(\Psi_k) \leq p$) .

In any case, designing S-tags is similar to the design of broad-band antennas, or even better of microwave filters, wherein frequency is replaced by the state of the process.

3.2 Global trade-off

In the most general case, the trade-off between communication and sensing is handled by performing a synthesis of the S-tag response $\xi \leftrightarrow \Psi$ by a proper shaping of the geometrical sizes $\mathbf{A} = \{a_1, .., a_K\}$ of the antenna, as for instance in the case of the profile of meander-line structures [22,23]

Such a problem can be formalized as the minimization with respect to $\mathbf{A}$ of a multi-objective function [24] like the following:

$$w_1 \sum_{m=1}^{M} |\xi([\Psi_m, \mathbf{A}]) - \xi_m| + w_2 \sum_{m=1}^{M} \frac{G_0}{G_T \tau[\Psi_m, \mathbf{A}]} \tag{16}$$

where (Ψ_m, ξ_m), $m = 1..M$, are control nodes of the sensing curve, e.g. the desired value of the antenna response at M realizations of the process, G_0 is the minimum realized gain in order to satisfy (14), and w_1 and w_2 are weights such that $w_1 + w_2 = 1$.

To reduce the degrees of freedom of the problem, the shape of the main radiator may be fixed (for instance a folded dipole or a PIFA) and the trade-off between communication and sensing is balanced through the shaping of an antenna adapter (Fig.5) in the form of a T-match, a Slot-match, a Loop-match or their variations as detailed described in [7]. In any case, above optimization problems can be conveniently solved by a stochastic tool such as the Genetic Algorithm [22] or the Particle Swarm [25].

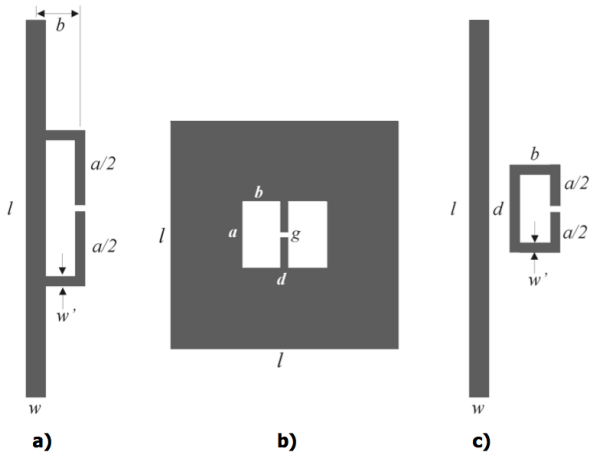

Figure 5: Typical layouts of antenna adapters used to control the impedance response of the tag. *a)* T-match, *b)* slot-match, *c)* loop-match.

3.3 $\{\tau[\Psi],\ AID[\Psi]\}$ Nomogram

Assuming the Analog Identifier in (6) as measurement metric, the relationship between the communication ($\tau[\Psi]$) and sensing ($AID[\Psi]$)

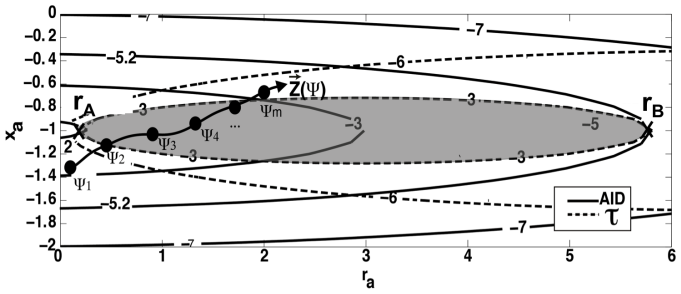

Figure 6: Iso-line of constant AID and τ on the normalized antenna impedance plane, for IC's quality factor Q=10. In grey the area corresponding to $\tau_{min} = -3dB$. The curve $\vec{Z}[\Psi] = r_a(\Psi)\hat{i} + x_a(\Psi)\hat{j}$ indicates a possible variation of the antenna's impedance all along the process in evolution.

parameters can be visually represented by a specific nomogram [24] that is useful to estimate the theoretical maximum dynamic range of the tag that can be achievable within the communication constraints in (14). At this purpose, power transmission coefficient and Analog Identifier are expressed in terms of normalized input impedance of the tag $r_a = R_A/R_{chip}, x_a = X_a/X_{chip}$, with $Q = |X_{chip}|/R_{chip}$ the quality factor of the chip:

$$\tau[\Psi] = \frac{4r_a}{|1 + r_a + jQ(1 + x_a)|^2} \tag{17}$$

$$\mathbf{AID}[\Psi] = \frac{2}{|1 + r_a + jQ(1 + x_a)|} = \sqrt{\frac{\tau}{r_a}} \tag{18}$$

Having fixed Q, a chart of {τ, AID} isolines is produced in decibel by varying r_a and x_a (Fig.6). Such lines are ellipses with major axis over $x_a = -1$ line and whose eccentricity depends on the quality factor Q of the microchip. The point $(r_a = 1, x_a = -1)$ corresponds to the *matched state* Ψ_M [19], e.g. the state of the process for which the tag's antenna shows the best matching to the IC: there, $Z_a = Z^*_{chip}$ and AID $= \tau = 0dB$.

The τ-AID nomogram does not depend on the particular antenna layout. The variation of the tag's impedance all along the phenomenon evolution can be therefore traced over such a plane by a sequence of couplets $\{r_a(\Psi_n), x_a(\Psi_n)\}$ describing an oriented curve (Fig.6):

$$\overrightarrow{Z}[\Psi] = r_a(\Psi)\hat{i} + x_a(\Psi)\hat{j} \in \mathbb{R}^2 \tag{19}$$

According to the intercepted isolines, the S-tag will show different sensing and communication behavior all along the process.

Communication constrains in (14) or in (15) become a condition over the power transfer coefficient

$$\tau[\Psi] \geq \frac{g}{G_T(\Psi)} \equiv \tau_{min} \tag{20}$$

Such a condition defines the region (shadowed in Fig.6) wherein the allowed dynamic range of the tag response has to be constrained. The maximum variation $\Delta \boldsymbol{AID}_{max}$ will be given by the AID isolines passed by the extremes $A = (r_A, -1), B = (r_B, -1)$ of the major axis of the $\tau = \tau_{min}$ ellipse. The multi-objective function to be minimized in (16) is hence reduced to a condition on the input impedance path $\overrightarrow{Z_m}[\Psi]$. The antenna's geometrical parameters **A** have to be **engineered in order to force the impedance curve to the straight segment $\overrightarrow{Z_m}[\Psi_m, \mathbf{A}] = \overline{AB}$. This means that the best sensing mechanism over the antenna is such to convert the variation of the process into a change of the only input resistance.**

The $\{\tau[\Psi],\ AID[\Psi]\}$ chart finally provides reference information about the best trade-off (see Fig.7) between the minimum acceptable read-range degradation all along the process, e.g. the minimum power transfer coefficient τ_{min}, and the maximum achievable sensing dynamic range of the measurable indicator $\Delta AID_{max}(\tau_{min})$. For instance the choice $\tau_{min} = -3dB$ will permit not to degrade the read range below the 70% of its maximum value corresponding, for example, to the initial (or final) state of the process. Accordingly, the theoretical maximum range of the tag's response will be $\Delta AID = 7.5dB$.

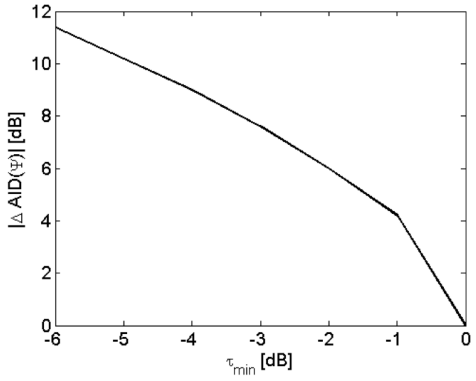

Figure 7: Maximum effective sensing capabilities of the radio-sensor for constant-gain process.

4 Bare S-Tags

Antennas are inherently sensitive to the change of the background medium. For instance, in case of a homogeneous space-filling material of parameters ($\mu = \mu_0\mu_r, \epsilon = \epsilon_0\epsilon_r$), the frequency dependence of its input impedance is shifted and scaled with respect to the air according to the Deschamps equation [26]

$$Z_A(\omega, \epsilon, \mu) = \sqrt{\frac{\mu_r}{\epsilon_r}} Z_A(\sqrt{\mu_r\epsilon_r}\omega, \epsilon_0, \mu_0) \tag{21}$$

In general, this phenomenon is usually considered as a limiting factor for RFIDs since, in order to optimize the tag, the material properties of the item to be tagged need to be known in advance. On the other hand, such performance variations can be interpreted as an intrinsic sensing capability. A modification of the tagged object is globally seen by the tag's antenna as a change of the surrounding equivalent permittivity, which in turn will produce a change of the tag's antenna impedance and received power (Fig.8a), and ultimately as a variation of the turn-on and backscattered power indicators. Therefore, a *self-sensing*, completely sensor-less, passive device is obtained wherein the *sensor is the antenna and the antenna is the sensor*. The same principle holds when the process under observation induces a deformation of the antenna shape, as in case of moving surfaces or evolving cracks. However this sensing mechanism is non-specific, since the sensed data may be only indirectly related to a physical phenomenon under observation.

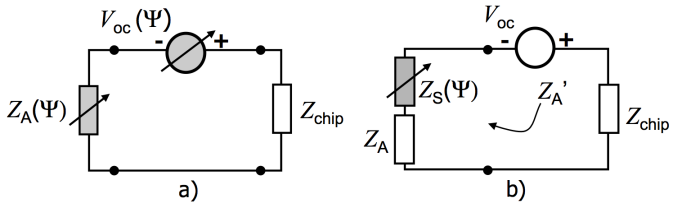

Figure 8: Equivalent receiving circuit for a) a bare tag whose antenna impedance and the open circuit induced voltage become dependent on the phenomenon Ψ under observation and b) for a tag whose antenna is loaded by a specific lumped sensor placed, for instance, in series with the RFID microchip.

4.1 Effective permittivity S-Tags

Fig.9 shows some examples of self-sensing tags recently proposed for remote observations of liquids, powders and biological processes. Each tag is documented with the achieved dynamic range and sensitivity as deduced by the original papers.

- a-b) Tags used as filling sensors for low-permittivity [15] and high-permittivity process [27]. The sensing activity can be performed by analyzing the variation of the reverse communication link, e.g the RSSI or equivalently the backscattered power of one or more tags matched at different filling levels. The same approach has been used in [28], for measuring urine volume in diapers primarily targeting infant and geriatric care applications. In this work the achieved dynamic range was R=7.8dB.

- c) An array of six commercially available RFID tags used as discrete detectors of the filling level of a bottle containing water [29]. Since the tags were tuned for operation in air, the ON state, e.g the ID transmission, occurs when there is no liquid around the tag, while the tag should remain silent when backed by water. By analyzing the specific set of IDs received by the reader, it is possible to retrieve the filling level of the container. The same approach has been used in [30] for providing an automatic warning system of running-out of injection fluid.

- d) A passive RFID bare sensor used also for detection of concrete water

infiltrations [31]. The presence of water sensibly changes the tag radiation and the matching performances of a tag drown in the concrete, up to completely detune it. A binary detection of water is thus proposed by relating the activation of the tag to the absence of water in its surrounding environment. More accurate and quantitative results may be achieved by considering customized RFID IC with three modulation states [32].

- e) **A passive RFID is used as a dielectric-property sensor for lightweight concrete. The tag is best matched for a dry condition of the concrete and experiences mismatch as the specimen exhibits different qualities due to the presence of water [33].**
- **f) A commercial tag used to monitor the level in a medical transfusion bag/bottle. The tag is tuned for operation in air and therefore is strongly detuned when the plastic bag/bottle is filled with transfusional liquid. The communication performance instead increase as the bag becomes empty [34].**
- g) A tag nested into a metallic structure, namely a cardiovascular stent. By adding the RFID IC, it is possible to transform the cardiovascular device into a radio-sensor able to monitor the restenosis process which induces a change in the properties of the material surrounding the tag [19].
- h) A dipole-like tag for detection of brain edema after surgical treatment for brain cancer [35]. Edema, which here roughly refers to water-imbued brain tissue, modifies the electromagnetic characteristics of the tissues surrounding a 1cm long implanted dipole tag, thus affecting the numerically computed two-way RFID link.

4.2 Deformation S-Tags

Some examples of tags recently developed to monitor deformations **and displacements** are shown in Fig. 10, with the corresponding ranges and sensitivities.

- a) A dipole-like tag, which can be ink-printed on fabric or on PVC. It can monitor the amount of deformation that it has undergone, by monitoring

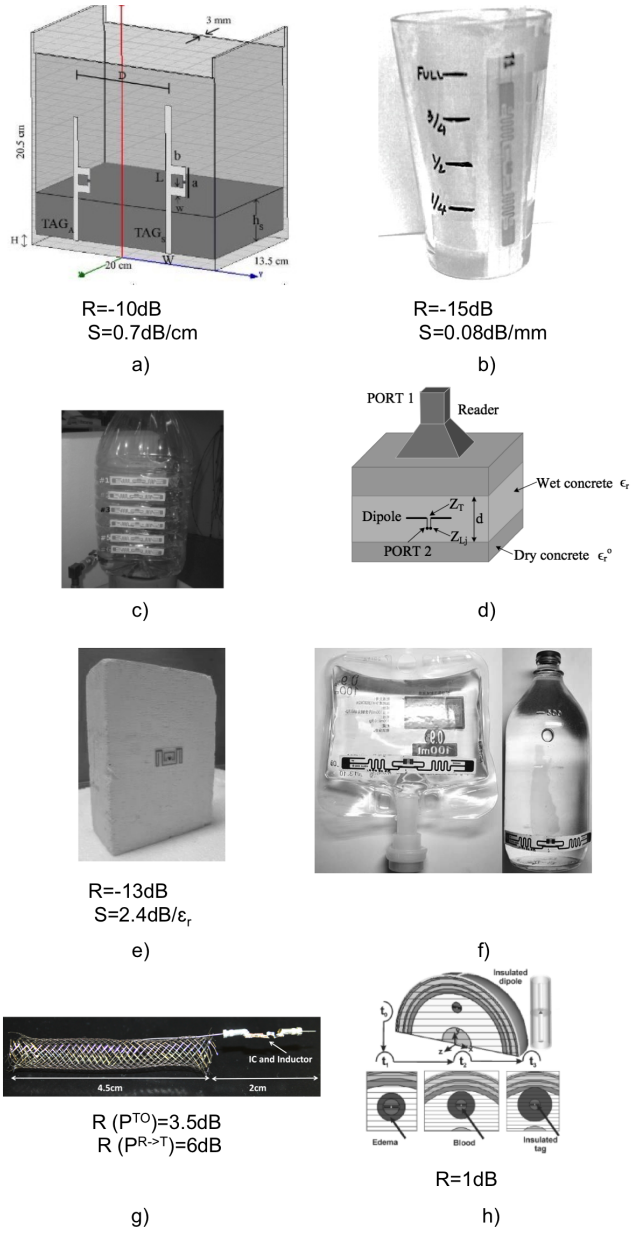

Figure 9: Examples of Effective-permittivity S-tags. a) Low-permittivity filling level sensor [15]; b) High- permittivity filling level sensor [27]; c) High-permittivity discrete filling level sensor [29]; d) Concrete water infiltration sensor [31]; e) Concrete humidity sensor[33]; f) High-permittivity filling level sensor [34] . Biological process sensors: f) the STENTag [19], g) Cerebral Edema monitoring [35].

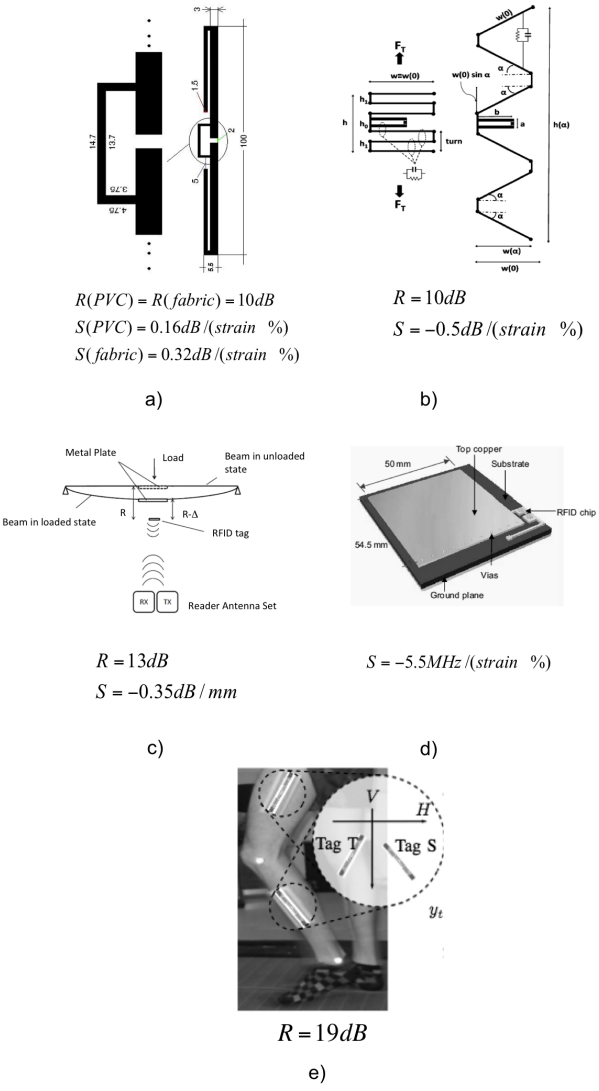

Figure 10: Examples of S-tags suitable to sense geometrical changes of objects. a) ink-printed stretchable folded dipole [17], b) flexible meander line antenna [36], c) proximity detuning by moving conductors [37] , d) deformable patch [38] e) Motion capture method [39].

the changes in the backscattered power, thanks to the changes in the effective conductivity of the ink when a strain is applied [17] .

- b) A meander-line antenna, designed to monitor strains. By applying an elongation, its shape will turn from a tightly-twisted meander to a zig-zag dipole, thus altering the antenna properties, such as the ratio of the actual backscattered power to the one measured during the steady state [36].

- c) A displacement sensor, obtained by exploiting the detuning characteristics of a metal plate behind a dipole-like tag. The metal plate is attached to the structural beam to be monitored and the RFID tag is placed in proximity to the metal plate facing the RFID reader. When loading occurs on the beam, a degradation of RFID tag performance is recordable at the reader, because of the destructive effect of the metal plane, now closer to the tag [37].

- d) A strain and crack sensor, by means of a folded patch antenna. The application of a tensile strain on the antenna results in a frequency shift of the turn on power, due to a longer electrical path [38].

- **e) A method for motion capture by using passive UHF linearly polarized tags properly placed on the human body segments. Dual polarized reader antennas are used to estimate the inclination of each tag based on the polarization of the tag responses [39].**

5 Loaded S-Tags

A more effective way to retrieve specific sensing data is to provide the tag with a "real" sensor which could be either lumped into a device [40, 41], connected in some part of the tag's antenna (Fig.8b) [42,43,44], or instead distributed all over the antenna surface, for instance as a chemical receptor painting [45]. The sensor is hence considered as a lumped or distributed impedance loading $Z_S(\Psi)$ on the tag's antenna. The variation of $Z_S(\Psi)$, caused by the change of the environment, will accordingly produce a change of the tag's gain and impedance, wirelessly detectable by measurement of the previously described indicators.

The design of such class of S-tags can be performed by the same approach as in (16) with the additional degrees of freedom of sensor displacement over the

antenna. It is worth noticing that this problem is similar to the design of loaded antennas, very popular in HF naval and vehicular communications to achieve broadband and multi-band communications. In that context, the position and number of loads (RLC circuits called "traps") are optimized by using a multi-port network representation of the antenna (see [46] for more details). A same idea could be in principle applied also to S-tag design. In the following sections, many examples are given, grouped according to the type of impedance loading.

5.1 Chemical loading

Kinds of S-tag loaded by chemical compounds are shown in Fig. 11.

- a) A first moisture sensor loaded by chemical species [47]. In this case the sensitive material is simply a blotting paper, eventually doped with NaCl (salt), covering an RFID patch-like tag. Since the paper absorbs water the radiation performances of the tag sensibly degrade, thus producing appreciable variations of the tag's response link.

- b) Loop-driven flat dipole doped with carbon nano structures (CNT), [45] able to sense the presence of ammonia in the environment thanks to the absorbing property of the CNT material deposited between the matching loop and the dipole. Changes in the CNT properties will reflect in mismatch and gain variation, readable through turn-on and backscattered power measurements.

- c) Tag connected to a one-way moisture sensor by means of a coupling loop. The printed sensor operates as a write-once-read-many (WORM) resistive memory device as it permanently changes its resistance from about $10k\Omega$ to 10Ω after exposure to moisture or water [18].

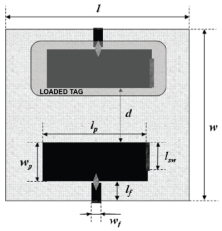

$\Delta RH = 50\%$
$R = 12dB$
$S_{low\ RH} = 0.13dB/\%RH$
$S_{high\ RH} = 0.3dB/\%RH$

a)

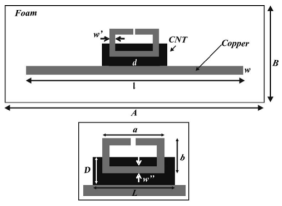

$R = 2dB$

b)

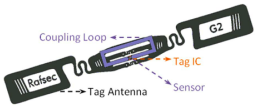

$\Delta RH \approx 30\%$
$R = 13dB$

c)

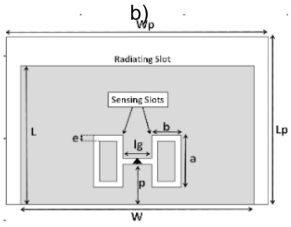

$\Delta RH = 50\%$
$R = 8dB$
$S_{low\ RH} = 0.18dB/\%RH$
$S_{high\ RH} = 0.13dB/\%RH$

d)

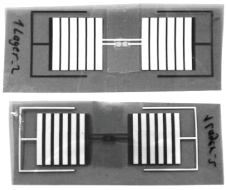

$\Delta RH \approx 100\%$
$S = 171KHz/\%RH$

e)

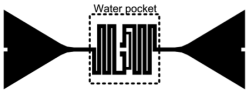

$\Delta T = 66°C$
$S = (729.5 \pm 7.5)KHz/°C$

f)

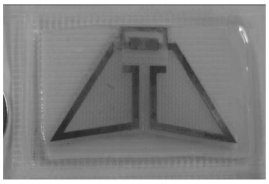

$\Delta T = 40°C$
$S = 0.1dB/°C$

g)

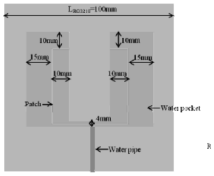

$\Delta T = 30°C$
$S = 0.6MHz/°C$

h)

Figure 11: Examples of Chemical Loaded Tags. a) Moisture Sensor integrating blotting paper [47] b) Ammonia Sensor integrating carbon nanotubes [45]; c) Humidity sensor integrating a resistive printed load [18]; d) Humidity Sensor integrating PEDOT:PSS [48]; e) Moisture sensor with sensitive dielectrics [49]; f) Temperature Sensor integrating distilled water [50]; g) Temperature sensor on paraffin wax [51]; h) Temperature sensor integrating a water pocket [52].

- d) Wearable tag [53] comprising a folded planar structure over a teflon substrate 4mm thick, provided with a radiating edge and a sensing H-shaped slot wherein gas-sensitive polymers can be spread. The material used in this work is the commercial species Clevios PH 500, a dispersion for conductive coatings with PEDOT and PSS. Like other polymers containing sulfonic acid groups, PEDOT:PSS is strongly hygroscopic and takes up moisture when handled under ambient conditions and consequently changes the Tag's radiation performances [48].

- e) Printed dipole loaded by distributed capacitors [49] for humidity sensing. The capacitors convert the permittivity variation of the substrate into a change in the antenna's impedance, remotely detectable through the frequency shift of the turn-on power measurements.

- f) Printed T-matched dipole-like tag loaded by distilled water encased within a plastic container and placed in close proximity to the impedance matching network [50]. The tag is capable of temperature monitoring. The varying electrical properties of the water alters the operation of the RFID tag itself throughout the impedance matching network. The turn-on power of the sensor experiences a frequency shift when measured at different temperatures.

- g) **Small tag printed on top of a multilayer substrate including paraffin wax for temperature monitoring. As temperature increases, the electrical properties of paraffin wax change, leading to mismatched operation for the tag and hence resulting into temperature sensing capabilities, through turn-on measurements [51].**

- **h) Patch-like tag printed on a multilayer substrate, including a small water pocket. Thanks to the change of water properties, the resonance of the tag shifts away along with temperature. It is possible to monitor temperature variations, while keeping a good reading range [52].**

5.2 Mechanical switch loading

Tags integrated with process-controlled switches have been mainly experienced for discrete sensing (Fig.**12),** e.g. with the purpose to detect and transmit the

occurrence of one or more specific states by ID modulation.

- a) Two-chip tag integrated with a temperature switch: one port of the tag is always active (i.e. it can be read at any temperature, giving the information of the tag's existence), while the other is shunted with a shape-memory alloy (SMAs) wire, which changes state at a given temperature, hence inhibiting or not the transmission of the code of the second chip [42].
- b) Dipole integrated with 1-bit accelerometer, obtained through the use of two mercury switches, each in series with one chip. By proper mounting of the switches, for instance in an antiparallel configuration, it is possible to achieve a "binary-code-shift keying", consisting in ID1 responding when the acceleration is parallel to the first switch and ID2 responding when acceleration is parallel to switch 2 [54].
- c) Wearable slotted-patch antenna integrated with an inertial omnidirectional switch that in rest state was demonstrated to exhibit a low inductive impedance while if subjected to motion, its impedance fluctuates between an ideal open circuit and the previous value [53].
- d) Another way to integrate a temperature switch into an RFID tag, by using shape memory polymers (SMP). Two different commercial tags are used, with a metal plate behind one of them, detuning it. When the temperature overcomes the threshold temperature, a shape-memory polymer moves the metal plate from one tag to the other's background, detuning the tag on front. In this way, different codes are transmitted to the reader in the two temperature states. A similar sensor is presented in [55], the actuator this time is an aqueous medium with a desired melting point. When the aqueous medium melts because of over-threshold temperature, the aluminum plate descends because of gravity, detuning the other tag and thus giving remotely the information of the critical state
- e) Two-state temperature-threshold detector tag [20]. The sensor is capable of relating the violation of a temperature threshold to a shift in the optimal operating frequency at which the tag antenna is well matched to the tag IC. The detuning mechanism consists of a metal plate placed behind the tag, whose distance can be controlled using a temperature-actuated switch, such as again a shape memory polymer (SMP).

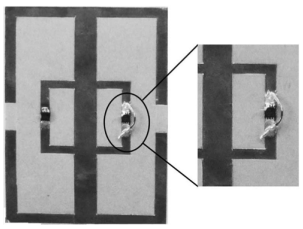

Temperature switch

a)

Acceleration switch

b)

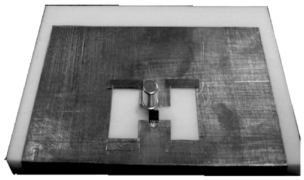

Motion switch

c)

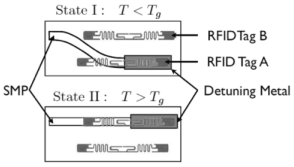

Temperature switch

d)

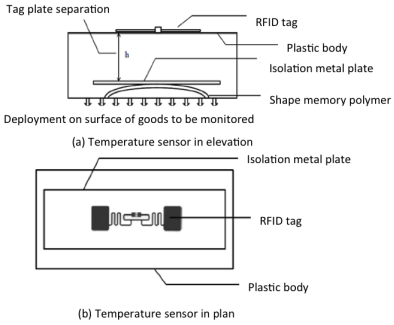

Temperature switch

e)

Figure 12: Examples of S-tags loaded with mechanical switches. a) temperature binary sensor integrating shape memory alloys [42]; b) acceleration binary sensor integrating an inertial switch [54]; c) motion binary sensor integrating an inertial switch [53] ; d) temperature binary sensor integrating a metal plate and shape memory alloys [55]; e) temperature binary sensor integrating a shape memory polymer [20].

For this family of S-Tags including multiple RFID ICs, the design challenge is to control in a selective way the responses of a highly-coupled multi-ports system wherein the behaviour of each tag is strongly related to the presence and on the status of the surrounding ones. The RFID GRID theory in [11, 12] provides all the required equations and procedures to manage multi-chip antennas which is a problem similar to the design of multi-ports loaded scatterers.

6 Fluctuations and Resolutions

The use of S-tags and readers for sensing measurements requires to face with fluctuations and discretization errors (see Fig. 13 for an example).

The fluctuation is produced by the internal noise of the receiver, by the limited stability of its components but also by the not stationary communication channel. The fluctuation may be partially reduced by performing a moving-window averaging over a dense set of samples.

The quantization error is instead related to the *resolution of the system*, e.g. the smallest detectable change (hereafter tagged by the symbol 'δ') of the quantity that it is being measured. Such variation $\delta\Psi$ may be written, after (12) as

$$\delta\Psi = \frac{\delta\xi}{S[\xi]} \tag{22}$$

The system resolution $\delta\Psi$ depends on the sensitivity of the S-Tag and on intrinsic features of the readers such as the voltage noise, the random fluctuation of the output signal, and on the quality of the receiving stage.

Finally, the number $n = \Delta\Psi/\delta\Psi$ of observable distinct states of the process between the extreme detectable values $(\Psi_{min}, \Psi_{min} + \Delta\Psi)$ will be therefore expressed in terms of the dynamic range, the S-tag sensitivity and the system resolution as

$$n = \frac{\Delta\xi}{\delta\Psi \cdot S[\xi]} = \frac{\Delta\xi}{\delta\xi} \tag{23}$$

The smallest appreciable variation $\delta\xi$ of the metrics introduced in the Section II will be detailed analyzed in the the following paragraphs.

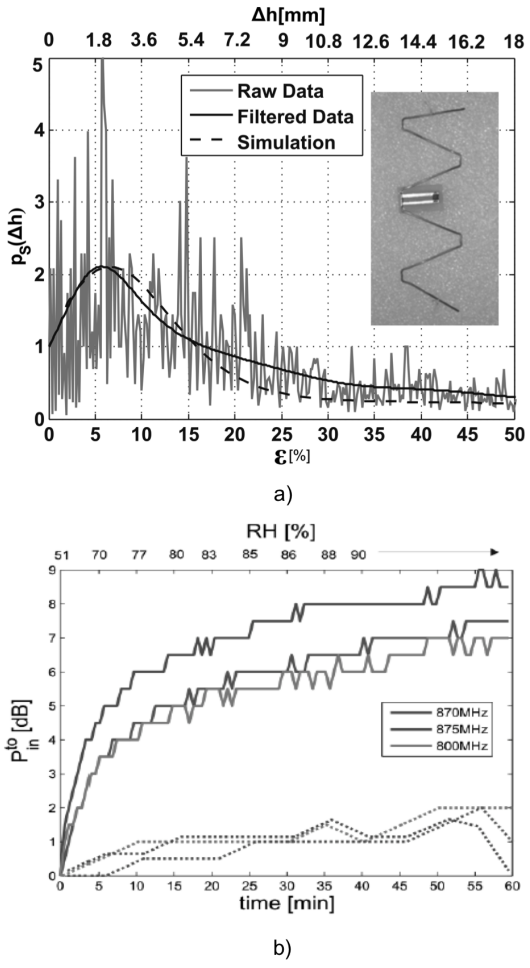

Figure 13: Examples of a) fluctuations of the received backscattered power (from [36]), and b) quantization error in the turn-on power (from [48])

6.0.1 Backscattered power ($\xi = P_{R\leftarrow T}$)

Having fixed the power emitted by the reader, then $\delta\xi|_{dB} = \delta P_{R\leftarrow T}|_{dB}$. This parameter depends on the power range of the reader's receiver and on the Analog to Digital Converter (ADC) discretizing the backscattered signal, e.g.

$$\delta P_{R\leftarrow T}|_{dB} = \frac{range|_{dB}}{2^N - 1} \tag{24}$$

where N is the number of ADC's bits. At the time of this writing, common available readers provide a received power resolution of the order of 1dB down to 0.1dB.

6.0.2 Turn-on power ($\xi = P_{in}^{to}$)

The resolution $\delta P_{in}^{to}|_{dB}$ corresponds to the minimum variation in the output power δP_{in}^{to} of the reader that can be controlled by the user. It is fixed by the manufacturer and it is again of the order of 0.1÷1dB.

6.0.3 AID ($\xi = AID$)

Having rewritten the Analog Identifier (6) in decibel ('dB' hereafter omitted to simplify notations)

$$AID = P_{chip} - \frac{1}{2}(P_{R\leftarrow T} + P_{in}^{to}) \tag{25}$$

the smallest appreciable variation occurs when only one or even both the two powers in (25) have changed by their minimum amount $\pm\delta P_{R\leftarrow T}$ and $\pm\delta P_{in}$, respectively. The minimum variation of AID may therefore fluctuate within the following set

$$|\delta AID_{min}| \in \{, \frac{|\delta P_{R\leftarrow T} \pm \delta P_{in}|}{2}, \frac{\delta P_{R\leftarrow T}}{2}, \frac{\delta P_{in}}{2}\} \tag{26}$$

and accordingly, the minimum resolution will be

$$|\delta AID_{min}| \leq \frac{\delta P_{R\leftarrow T} + \delta P_{in}}{2} \tag{27}$$

For example, a reader with $\delta P_{in} = 0.5dB$ and $\delta P_{R\leftarrow T} = 0.8dB$, will enable a resolution $|\delta\text{AID}|\leq 0.65dB$, thus better than the resolution over the backscattered power. Assuming an equal dynamic range $\Delta\xi = 3dB$ for all the three above metrics, then according to (23) the number of detectable states of the

Table 2: Examples of S-tag's performances

sensor	$\Delta\xi$ **(dB)**	S	$\delta\xi$ **(dB)**		n
Humidity [**?**]	12	0.3dB/RH%	1		12
			0.5		24
			0.1		120
Strain [**?**]	10	0.5dB/ϵ%	1		10
			0.5		20
			0.1		100
Level [**?**]	15	0.08dB/mm	1		15
			0.5		30
			0.1		150

process will be $n[P_{in}^{to}] = 6$, $n[P_{R\leftarrow T}] = 3$, and $n[AID] = 4$.

Table II shows some examples of estimated overall system performance for S-tag able to sense humidity, strain and filling level, with respect to the resolution of the readers' receiver. It can be noted that a resolution of $\delta\xi < 0.5dB$ could easily guarantee the discrimination of more than 20 grades of the process.

7 Emerging sensing paradigms

An emerging passive sensing architecture considers the RFID tag as a true data-logger: physical information collected by a specific sensor are handled by a micro controller, sampled and encoded into digital information that can be stored in the microchip's memory and then recovered by the reader through regular RFID interrogation. These objects are usually battery-assisted and hence they act as semi-active devices. However, if the micro-controller requires very low power consumption (a few milliwatts), the energy required to drive the data acquisition may be directly harvested out of some cycles of the interrogation signal or generated by piezo-electric energy scavengers or by solar panels. A super-capacitor is hence required for energy storage. Examples of this class of devices are the WISP [56] and the platform in [57], which can both be integrated with general-purpose sensors. The former device codes the measured data into the ID transmitted by the tag, the latter one is instead a battery assisted multi-ID tag and it is capable to transmit, when interrogated by a standard RFID reader, a proper combination of ID codes that univocally represents the measured value.

Off the shelf RFID ICs with augmented sensing capabilities are nowadays available [58, 59]. They include high speed non-volatile memory (EEPROM),

typically integrate an embedded temperature sensor and provide programmable I/O ports for connecting general purposes micro controllers and sensors as in [60]. These devices can be considered as a convergence point among fully passive tags, as those described in this paper, and the autonomous sensor nodes having local computational capability. Indeed they could be practically immune to the environment interactions and the onboard sensors can be moreover extremely specific. Thus they could provide a possible trade-off between superior sensing performance and cost. The electromagnetic challenge is rather small since the sensing and communication functionalities are fully decoupled.

8 Conclusion

The applicability of the RFID technology to passive sensing is now a fact, demonstrated by many independent researches worldwide. Many more examples are expected to come in the next years, stimulated by the virtuous interaction among different expertises. In particular RFID chemical sensors could have a great commercial interest thanks to the fabrication simplicity and to the potential mass diffusion in food and pharma control chains.

Anyway, the design of S-tags is not yet a mature discipline since unified methodologies are still required to efficiently handle multi-physics optimization and data processing. This is a kind of short-range sensing, therefore it is expected that some methods will be borrowed from the more assessed and mature Remote Sensing background.

Sensitivity and resolution of the reader are currently the main bottleneck of the passive S-tags technology. These critical issues are expected to be mitigated in the future generations of readers (mainly by increasing the analog-to-digital converter performance). The concurrent reduction of the chip sensitivity will enable a close integration of this technology in general-purpose smartphones with unpredictable applications in the distributed or ubiquitous computing boosting the evolution of the Internet of Things.

At the very end, being now available the new all-on-chip multifunction components described in Session VII which at most require only external storage capacitors and promise high sensing accuracy, it is now paradoxically necessary to rise the question whether to continue making research on completely passive radio-sensors involving less accurate and still challenging analog reading. The answer is not univocal and can not be kept separate from the application

fields. All those sensors *disappearing into things* (as claimed by Mark Wiser in his popular essay on "The Computer for the 21st Century" [61], e.g. for really massive and pervasive applications), require to be as simple, cheap and small as possible, and hence the research on sensitive antennas, with a so big physical insight, definitely keeps on making sense. For biomedical applications, completely passive radio-sensors are useful as well to enable the widespread diffusion of smart disposable devices, e.g plasters enhanced with sensing and communication functionalities. For integration with implantable devices, the possibility to avoid batteries and additional components will simplify the bio-compatibility of the radio-sensor and such advantage overcomes the eventual drawbacks related to low resolution. Sporadic placements, for instance in case of precise environmental monitoring wherein the accuracy of the measurement is the main requirement but the read distance is not a particular issue, will instead greatly take benefit of battery- or capacitor-assisted RFID IC, which could be a strategic choice as the short-range version of the more complex but powerful autonomous sensor nodes.

References

[1] D. M. Dobkin, The RF in RFID: passive UHF RFID in Practice. Amsterdam: Elsevier, 2007.

[2] L. Atzori, A. Iera, and G. Morabito, "The internet of things: A survey," Computer Networks, vol. 54, no 15, pp. 2787 – 2805, 2010. [Online]. Available: http://www.sciencedirect.com/science/article/pii/S1389128610001568

[3] J. Rabaey, "The swarm at the edge of the cloud - a new perspective on wireless," in VLSI Circuits (VLSIC), 2011 Symposium on, june 2011, pp. 6 –8.

[4] R. Bhattacharyya, C. Floerkemeier, and S. Sarma, "Low-cost, ubiquitous rfid-tag-antenna-based sensing," Proceedings of the IEEE, vol. 98, no. 9, pp. 1593 –1600, sept. 2010.

[5] B. Warneke, M. Last, B. Liebowitz, and K. Pister, "Smart dust: communicating with a cubic-millimeter computer," Computer, vol. 34, no. 1, pp. 44 –51, jan 2001. 30

[6] L. Theremin, "Signaling apparatus," February 1928.

[7] G. Marrocco, "The art of uhf rfid antenna design: impedance-matching and size-reduction techniques," Antennas and Propagation Magazine, IEEE, vol. 50, no. 1, pp. 66 –79, feb. 2008.

[8] G. Marrocco, "Pervasive electromagnetics: sensing paradigms by passive rfid technology," Wireless Communications, IEEE, vol. 17, no. 6, pp. 10 –17, december 2010.

[9] EPC Radio-Frequency Identity Protocols Class-1 Generation-2 UHF RFID Protocol for Communications at 860 MHz - 960 MHz, http://www.gs1.org/gsmp/kc/epcglobal/uhfc1g2/.

[10] G. Marrocco, L. Mattioni, and C. Calabrese, "Multiport sensor rfids for wireless passive sensing of objects: Basic theory and early results," Anten nas and Propagation, IEEE Transactions on, vol. 56, no. 8, pp. 2691 –2702, aug. 2008.

[11] G. Marrocco, "Rfid grids: Part i:electromagnetic theory," Antennas and Propagation, IEEE Transactions on, vol. 59, no. 3, pp. 1019 –1026, march 2011.

[12] S. Caizzone and G. Marrocco, "Rfid grids: Part ii: Experimentations," Antennas and Propagation, IEEE Transactions on, vol. 59, no. 8, pp. 2896 –2904, aug. 2011.

[13] P. Nikitin and K. Rao, "Theory and measurement of backscattering from rfid tags," Antennas and Propagation Magazine, IEEE, vol. 48, no. 6, pp. 212 –218, dec. 2006.

[14] F. Fuschini, C. Piersanti, F. Paolazzi, and G. Falciasecca, "Analytical approach to the backscattering from uhf rfid transponder," Antennas and Wireless Propagation Letters, IEEE, vol. 7, pp. 33 –35, 2008.

[15] G. Marrocco and F. Amato, "Self-sensing passive rfid: From theory to tag design and experimentation," in European Microwave Conference, 2009. EuMC 2009. oct. 2009, pp. 001 –004.

[16] J. Bolomey, S. Capdevila, L. Jofre, and J. Romeu, "Electromagnetic model- ing of rfid-modulated scattering mechanism. application to tag performance evaluation," Proceedings of the IEEE, vol. 98, no. 9, pp. 1555 –1569, sept. 2010.

[17] S. Merilampi, P. Ruuskanen, T. Bjorninen, L. Ukkonen, and L. Sydanheimo, "Printed passive uhf rfid tags as wearable strain sensors," in Applied Sciences in Biomedical and Communication Technologies (ISABEL), 2010 3rd International Symposium on, nov. 2010, pp. 1 –5.

[18] J. Gao, J. Siden, and H.-E. Nilsson, "Printed electromagnetic coupler with an embedded moisture sensor for ordinary passive rfid tags," Electron Device Letters, IEEE, vol. 32, no. 12, pp. 1767 –1769, dec. 2011.

[19] Occhiuzzi, C.; Contri, G.; Marrocco, G.; , "Design of Implanted RFID Tags for Passive Sensing of Human Body: The STENTag," Antennas and Prop-

agation, IEEE Transactions on , vol.60, no.7, pp.3146-3154, July 2012

[20] R. Bhattacharyya, C. Floerkemeier, S. Sarma, and D. Deavours, "Rfid tag antenna based temperature sensing in the frequency domain," in RFID (RFID), 2011 IEEE International Conference on, april 2011, pp. 70 –77.

[21] S. Caizzone, C. Occhiuzzi, and G. Marrocco, "Multi-chip rfid antenna inte- grating shape-memory alloys for detection of thermal thresholds," Antennas and Propagation, IEEE Transactions on, vol. PP, no. 99, p. 1, 2011.

[22] G. Marrocco, "Gain-optimized self-resonant meander line antennas for rfid applications," Antennas and Wireless Propagation Letters, IEEE, vol. 2, no. 1, pp. 302 –305, 2003.

[23] C. Calabrese and G. Marrocco, "Meandered-slot antennas for sensor-rfid tags," Antennas and Wireless Propagation Letters, IEEE, vol. 7, pp. 5 –8, 2008.

[24] C. Occhiuzzi and G. Marrocco, "Electromagnetic optimization of passive rfid sensor nodes," in Antennas and Propagation (EuCAP), 2012 Proceedings of the Sixth European Conference on, 2012, pp. 70 –77.

[25] J. Robinson and Y. Rahmat-Samii, "Particle swarm optimization in electromagnetics," Antennas and Propagation, IEEE Transactions on, vol. 52, no. 2, pp. 397 – 407, feb. 2004.

[26] G. Deschamps, "Impedance of an antenna in a conducting medium," Antennas and Propagation, IRE Transactions on, vol. 10, no. 5, pp. 648 –650, september 1962.

[27] R. Bhattacharyya, C. Floerkemeier, and S. Sarma, "Rfid tag antenna based sensing: Does your beverage glass need a refill?" in RFID, 2010 IEEE International Conference on, april 2010, pp. 126 –133.

[28] H.-E. Nilsson, J. Siden, and M. Gulliksson, "An incontinence alarm solution utilizing rfid based sensor technology," in RFID-Technologies and Applications (RFID-TA), 2011 IEEE International Conference on, sept. 2011, pp. 359 –363.

[29] S. Capdevila, L. Jofre, J. Romeu, and J. Bolomey, "Passive rfid based sensing," in RFID-Technologies and Applications (RFID-TA), 2011 IEEE International Conference on, sept. 2011, pp. 507 –512.

[30] C.-F. Huang and J.-H. Lin, "A warning system based on the rfid technology for running-out of injection fluid," in Engineering in Medicine and Biology Society,EMBC, 2011 Annual International Conference of the IEEE, 30 2011-sept. 3 2011, pp. 2212 –2215.

[31] S. Capdevila, G. Roqueta, M. Guardiola, L. Jofre, J. Romeu, and J. C. Bolomey, "Water infiltration detection in civil engineering structures using

rfid," in Antennas and Propagation (EUCAP), 2012 6th European Conference on, march 2012, pp. 2505 –2509.

[32] S. Capdevila, L. Jofre, J.-C. Bolomey, and J. Romeu, "Rfid multi- probe impedance-based sensors," Instrumentation and Measurement, IEEE Transactions on, vol. 59, no. 12, pp. 3093 –3101, dec. 2010.

[33] R. Suwalak, C. Phongcharoenpanich, D. Torrungrueng, and M. Krairiksh, "Determination of dielectric property of construction material products us- ing a novel rfid sensor," Progress In Electromagnetics Research, vol. 130, pp. 601–617, 2012.

[34] Z. Jiang, Z. Fu, and F. Yang, "Rfid tag antenna based wireless sensing method for medical transfusion applications," in RFID-Technologies and Applications (RFID-TA), 2012 IEEE International Conference on, sept. 2012. 33

[35] C. Occhiuzzi and G. Marrocco, "Sensing the human body by implanted rfid tags," in Antennas and Propagation (EuCAP), 2010 Proceedings of the Fourth European Conference on, april 2010, pp. 1 –5.

[36] C. Occhiuzzi, C. Paggi, and G. Marrocco, "Passive rfid strain-sensor based on meander-line antennas," Antennas and Propagation, IEEE Transactions on, vol. 59, no. 12, pp. 4836 –4840, dec. 2011.

[37] R. Bhattacharyya, C. Floerkemeier, and S. Sarma, "Towards tag antenna based sensing - an rfid displacement sensor," in RFID, 2009 IEEE Inter- national Conference on, april 2009, pp. 95 –102.

[38] X. Yi, C. Cho, C.-H. Fang, J. Cooper, V. Lakafosis, R. Vyas, Y. Wang, R. T. Leon, and M. M. Tentzeris, "Wireless strain and crack sensing using a folded patch antenna," in Antennas and Propagation (EUCAP), 2012 6th European Conference on, march 2012, pp. 1678 –1681.

[39] R. Krigslund, S. Dosen, P. Popovski, J. Dideriksen, G. Pedersen, and D. Farina, "A novel technology for motion capture using passive uhf rfid tags," Biomedical Engineering, IEEE Transactions on, vol. PP, no. 99, p. 1, 2012.

[40] C. Occhiuzzi and G. Marrocco, "The rfid technology for neurosciences: Feasibility of limbs' monitoring in sleep diseases," Information Technology in Biomedicine, IEEE Transactions on, vol. 14, no. 1, pp. 37 –43, jan. 2010.

[41] A. Vaz, A. Ubarretxena, I. Zalbide, D. Pardo, H. Solar, A. Garcia-Alonso, and R. Berenguer, "Full passive uhf tag with a temperature sensor suitable for human body temperature monitoring," Circuits and Systems II: Express Briefs, IEEE Transactions on, vol. 57, no. 2, pp. 95 –99, feb. 2010.

[42] S. Caizzone, C. Occhiuzzi, and G. Marrocco, "Multi-chip rfid antenna integrating shape-memory alloys for detection of thermal thresholds," Antennas

and Propagation, IEEE Transactions on, vol. 59, no. 7, pp. 2488 –2494, july 2011.

[43] J. Virtanen, L. Ukkonen, T. Bjorninen, A. Elsherbeni, and L. Sydanheimo, "Inkjet-printed humidity sensor for passive uhf rfid systems," Instrumentation and Measurement, IEEE Transactions on, vol. 60, no. 8, pp. 2768 –2777, aug. 2011. 34

[44] L. Yang, R. Zhang, D. Staiculescu, C. Wong, and M. Tentzeris, "A novel conformal rfid-enabled module utilizing inkjet-printed antennas and carbon nanotubes for gas-detection applications," Antennas and Wireless Propagation Letters, IEEE, vol. 8, pp. 653 –656, 2009.

[45] C. Occhiuzzi, A. Rida, G. Marrocco, and M. Tentzeris, "Rfid passive gas sensor integrating carbon nanotubes," Microwave Theory and Techniques, IEEE Transactions on, vol. PP, no. 99, p. 1, 2011.

[46] L. Mattioni and G. Marrocco, "Blade: A broadband loaded antenna designer," Antennas and Propagation Magazine, IEEE, vol. 48, no. 5, pp. 120 –129, oct. 2006.

[47] S. Johan, X. Zeng, T. Unander, A. Koptyug, and H.-E. Nilsson, "Remote moisture sensing utilizing ordinary rfid tags," in Sensors, 2007 IEEE, oct. 2007, pp. 308 –311.

[48] S. Manzari, C. Occhiuzzi, S. Nawale, A. Catini, C. Di Natale, and G. Marrocco, "Humidity sensing by polymer-loaded uhf rfid antennas," Sensors, IEEE, 2012.

[49] J. Virtanen, L. Ukkonen, T. Bjoandrninen, A. Z. Elsherbeni, and L. Sydaandnheimo, "Inkjet-printed humidity sensor for passive uhf rfid systems," Instrumentation and Measurement, IEEE Transactions on, vol. PP, no. 99, pp. 1 –10, 2011.

[50] J. Virtanen, L. Ukkonen, T. Bjorninen, L. Sydanheimo, and A. Elsherbeni, "Temperature sensor tag for passive uhf rfid systems," in Sensors Applications Symposium (SAS), 2011 IEEE, feb. 2011, pp. 312 –317.

[51] A. Babar, S. Manzari, L. Sydanheimo, A. Elsherbeni, and L. Ukkonen, "Passive uhf rfid tag for heat sensing applications," Antennas and Propagation, IEEE Transactions on, vol. 60, no. 9, pp. 4056 –4064, sept. 2012.

[52] Q. Qiao, F. Yang, and A. Elsherbeni, "Read range and sensitivity study of rfid temperature sensors," in Antennas and Propagation Society International Symposium (APSURSI), 2012 IEEE, july 2012, pp. 1 –2.

[53] C. Occhiuzzi, S. Cippitelli, and G. Marrocco, "Modeling, design and experimentation of wearable rfid sensor tag," Antennas and Propagation, IEEE

Transactions on, vol. 58, no. 8, pp. 2490 –2498, aug. 2010. 35

[54] M. Philipose, J. Smith, B. Jiang, A. Mamishev, S. Roy, and K. Sundara-Rajan, "Battery-free wireless identification and sensing," Pervasive Computing, IEEE, vol. 4, no. 1, pp. 37 – 45, jan.-march 2005.

[55] R. Bhattacharyya, C. Floerkemeier, and S. Sarma, "Rfid tag antenna based temperature sensing," in RFID, 2010 IEEE International Conference on, april 2010, pp. 8 –15.

[56] A. Sample, D. Yeager, P. Powledge, and J. Smith, "Design of a passively-powered, programmable sensing platform for uhf rfid systems," in RFID, 2007. IEEE International Conference on, march 2007, pp. 149 –156.

[57] L. Catarinucci, R. Colella, and L. Tarricone, "A cost-effective uhf rfid tag for transmission of generic sensor data in wireless sensor networks," Microwave Theory and Techniques, IEEE Transactions on, vol. 57, no. 5, pp. 1291 – 1296, may 2009.

[58] [Online]. Available: EM 4325, at www.emmicroelectronic.com

[59] [Online]. Available: NXP Ucode I2C www.nxp.com

[60] T. Unander, J. Siden, and H.-E. Nilsson, "Designing of rfid-based sensor solution for packaging surveillance applications," Sensors Journal, IEEE, vol. 11, no. 11, pp. 3009 –3018, nov. 2011.

[61] M. Weiser, "The computer for the 21st century," pp. 933–940, 1995.

Cecilia Occhiuzzi (M'12) received the M.Sc. degree in medical engineering and the Ph.D. in electromag- netics from the University of Rome "Tor Vergata", in 2008 and 2011, respectively. Currently, she is a Research Assistant in the University of Rome "Tor Vergata", with interests in wireless health monitoring by means of wear- able and implantable radiofrequency identification techniques. In 2008, she was with the School of En- gineering, University of Warwick, Warwick, U.K., as a postgraduate student involved with design and implementation of wireless surface acoustic wave (SAW) sensors. In 2010, she was a Visiting Researcher with the Georgia Institute of Technology, Atlanta. Her research was mainly focused on the design of passive RFID sensors for structural health monitoring and gas detection by means of CNT-based tags. She holds two patents on sensor RFID systems.

Stefano Caizzone received the M.Sc. degree in Telecommunications Engineering from the University of Rome "Tor Vergata" in 2009 and he is currently part-time working toward the Ph.D. degree. His main research interests concern small antennas for RFIDs and navigation, antenna arrays and grids with enhanced sensing capabilites. He is now with the Antenna group of the Institute of Communications and Navigation of the German Aerospace Center (DLR), Wessling, Germany, where he is responsible for the development of innovative miniaturized antennas.

Gaetano Marrocco was born in Teramo, Italy, on August 29, 1969, He received the Laurea degree in Electronic Engineering (Laurea cum Laude and Academic Honour) and the Ph.D. degree in Applied Electromagnetics from the University of L'Aquila, Italy, in 1994 and 1998, respectively. Since 1997, he has been a Researcher at the University of Rome "TorVergata," Rome, Italy, where he currently teaches Electromagnetic Technology for Wireless Systems and Medical Radio-Systems, manages the Pervasive Electromagnetics Lab and is advisor in the Geo-Information PhD program. In October 2010 he achieved the degree of Associate Professor of Electromagnetic.
In 1994, he was at the University of Illinois at Urbana-Champain as a

Postgraduate Student. In 1999, he was a Visiting Researcher at the Imperial College in London, U.K. In 2008 he joined the PhD program of the University of Grenoble (FR).
His research is mainly directed to the modeling and design of broadband and ultra wideband (UWB) antennas and arrays as well as of sensor-oriented miniaturized antennas for Biomedicine, Aeronautics and Radiofrequency Identification (RFID).
Prof. Marrocco has been involved in several Space, Avionic, Naval and Vehicular programs of the European Space Agency, NATO, Italian Space Agency, and the Italian Navy about the analysis and the design of non-conventional antennas and systems over platforms.
He submitted eight patents on broadband naval antennas and structural arrays, and on sensor RFID systems.
Currently, he serves as Associate Editor of the IEEE Antennas and Wireless Propagation Letters, Vice-Chair of the Italian delegation URSI Commission D: Electronics and Photonics, and as member of Technical Program Committee of IEEE RFID, IEEE IMS and ISABEL.
In 2008 he was the General Chairman of the first Italian multidisciplinary scientific workshop on RFID: RFIDays-2008: Emerging Technology for Radiofrequency Identification. He was the co-chair of the RFIDays-2010 International Workshop in Finland and Chairman of the Local Committee of the V European Conference on Antennas and Propagation and TCP chair of the 2012 IEEE-RFID TA in Nice, France.